SUPPLEMENT TO THE *WELDING JOURNAL*, JULY 2011
**Sponsored by the American Welding Society and the Welding Research Council**

# Effect of Tool Geometries on Thermal History of FSW of AA1100

*The peak temperatures measured, which have major influence on the overall welding process, were found to be in very good agreement with the calculated values*

**BY P. BISWAS AND N. R. MANDAL**


## ABSTRACT

In the present work, three-dimensional finite element (FE) transient thermal analysis of friction stir welding (FSW) was presented for different tool geometries and different process parameters. The source of heat generation was assumed to be pure friction between the tool and workpiece interface. Thermal history of FSW of 6-mm-thick AA1100 plates for different tool geometries was calculated. The estimated thermal profiles compared well with those of the experimental results, thus validating the various assumptions made in the work. It was observed that in FSW of AA1100 with SS310 tool, friction is the major contributor to heat generation. Tool geometry with concave shoulder and conical pin was found to be preferable for FSW of AA 1100. It is preferable to keep the tool pin diameter as small as possible to avoid occurrence of a wormhole defect. Tool plunging force reduced significantly with an increase in tool rotational speed; however, the increase in heat generation was marginal.


## Introduction

Friction stir welding (FSW) is a solid-state joining technique. The welds are created by the combined action of frictional heating and mechanical deformation due to a rotating tool. The majority of the heat generated from the friction, i.e., about 95%, is transferred into the workpiece and only 5% flows into the tool (Ref. 1). The maximum temperature created by the FSW process ranges from 80 to 90% of the melting temperature of the material being welded.

The localized heating softens the material around the pin. Tool rotation and translation leads to movement of material from the front of the pin to the back of the pin. As a result of this process, a joint is produced in the solid state. Plastic flow in FSW is a complex phenomenon due to the interaction of the variation of strain rates and flow stress leading to variation in viscosity, which affects the flow (Ref. 2). Because of various geometrical features of the tool, the material movement around the pin can be quite complex (Ref. 3). Design of tools based on quantitative understanding of material flow is just beginning (Ref. 2). Colegrove and Shercliff (Refs. 4, 5) suggested that Trivex™ tools with their convex surfaces avoid sticking to the material, thus reducing the shear force at the tool-metal interface, leading to reduction in traverse force. However, at the same time, they observed that the heat generated, as well as the power requirement, remained unchanged by different tool designs. During FSW, the material undergoes intense plastic deformation at elevated temperature, resulting in generation of fine and equiaxed recrystallized grains (Ref. 6). The fine microstructure in friction stir welds results in improved mechanical properties.


## KEYWORDS

Finite Element Analysis
Transient Thermal Analysis
Friction Stir Welding
Temperature-Dependent Material Properties
Tool Geometries


*P. BISWAS* (panu012@yahoo.co.in) *is research associate and N. R. MANDAL* (nrm@naval.iitkgp.ernet.in) *is professor, Department of Ocean Engineering and Naval Architecture, Indian Institute of Technology, Kharagpur, India.*

In FSW, there are two sources of heat generation. One through friction and the other due to plastic deformation at the tool-workpiece interface and at the thermomechanically-affected zone (TMAZ) (Refs. 7–9). The tool-workpiece interface can be further subdivided into shoulder-workpiece and tool pin-workpiece interface. In most models (Refs. 10–16), heat generated from the tool pin was neglected.

Ulysse (Ref. 17) presented a 3D finite element model for determining the temperature profile using a commercial FEM (finite element method) code FIDAP. The heat generation rate was expressed as the product of the effective flow stress and the effective strain rate. Reasonable agreement between the predicted and the measured temperature was reported.

Chen and Kovacevic (Ref. 18) developed a 3D finite element model to study the thermal history and thermomechanical phenomena in butt-joint welding of aluminum Alloy 6061-T6 using a commercial FEM code ANSYS. Their model incorporated the mechanical reaction between the tool and the weld material. X-ray diffraction technique was used to measure the residual stress in the welded plate.

A few models did consider the effect of tool pin on heat generation (Refs. 19–21). For instance, in Colegrove et al. (Ref. 19) 20% of the total heat was attributed to the pin, yet, they concluded that the addition of heat due to the pin had little effect on the thermal profile produced from the modeling. However, tool pin geometry was not given in the report. The relative contributions of the heat generated from these two sources remained unknown.

Nandan et al. (Refs. 22, 23) combined viscoplastic flow with heat transfer to study the three-dimensional FSW process in 6061 aluminum alloy. They (Ref. 24) further expanded the study to mild steel. Although they claimed that the computed temperatures were in good agreement with the corresponding experimentally determined values, only temperatures at one

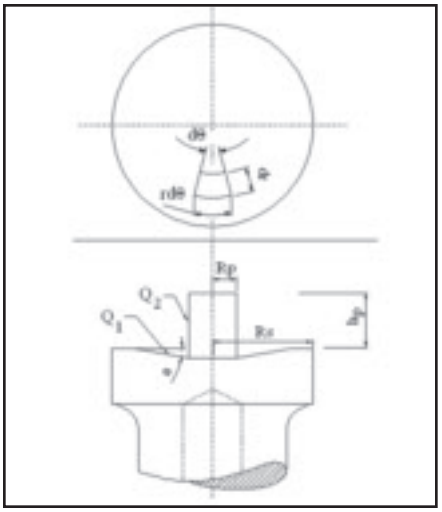

*Fig. 1 — Segmental areas and heat generation on different parts of the FSW tool.*

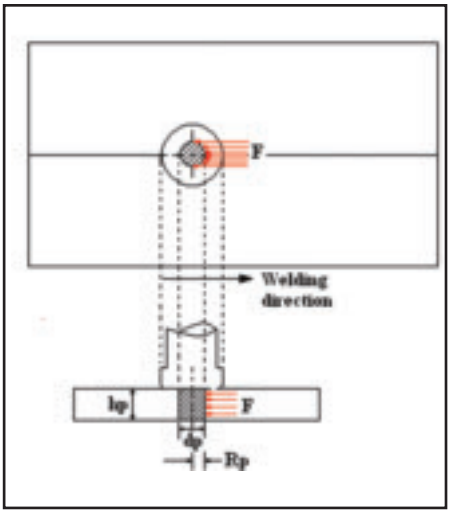


*Fig. 2 — Force acting on FSW tool pin due to welding.*

remote point from the tool were reported (Ref. 24).

The works of the above investigators indicate that the heat generation and the resulting thermal history in a FSW process are greatly influenced by tool rotational speed and to a much lesser extent by the tool traverse speed. Not much information on the effect of tool geometry, including that of tool pin on thermal profile, was reported in the literature. The present study therefore focused primarily on the effect of variation of tool geometry on thermal profile. Extensive experiments were carried out to test the simulation results.

## Heat Generation

In FSW, heat is generated due to friction and plastic deformation at the tool-workpiece interface and at the TMAZ. The heat generation at the contact surfaces due to friction is the product of frictional force and the tangential speed of the tool with respect to the workpiece. The heat generated per unit area due to plastic deformation at the tool-workpiece interface is the product of shear stress and the velocity of the workpiece material sticking to the tool as it traverses. This velocity is actually the tangential speed of the tool.

The heat generation due to friction on an elemental area $dA$ at the tool-workpiece interface, considering high rotational speed compared to traverse speed of the FSW tool, is given by

$$dQ_f = (1-\delta)\omega r \mu p dA \qquad (1)$$

The heat generated due to plastic shear deformation leading to workpiece material sticking to the tool is given by

$$dQ_p = \delta \omega r \tau_y dA \qquad (2)$$

Therefore, total heat due to friction and plastic deformation is given by

$$\begin{aligned} dQ &= dQ_f + dQ_p \\ &= \omega r dA(\mu p - \delta \mu p) + \delta \tau_y \\ \text{Let } \tau_{contact} &= \left[(\mu p - \delta \mu p) + \delta \tau_y\right] \end{aligned} \qquad (3)$$

$$\text{Therefore, } dQ = \omega r dA \tau_{contact} \qquad (4)$$

There is no straightforward mechanism to estimate the extent of slip. At the same time, with the increase in temperature, the yield strength of the workpiece material decreases, resulting in reduction in heat generation from plastic deformation. In such a situation, it was felt more logical to consider pure friction and neglect the heat generation due to plastic deformation. In the case of pure friction $\delta = 0$. Therefore, Equation 3 reduces to

$$\tau_{contact} = \mu p \qquad (5)$$

Therefore, from Equations 4 and 5, the expression for heat generation on an elemental surface area $dA$ at the tool-workpiece interface is given by

$$\begin{aligned} & dQ = \omega r\ \mu p\ dA \\ \text{i.e.,} \quad & dQ = \omega r\ dF \\ \text{where} \quad & dF = \mu p\ dA \end{aligned} \qquad (6)$$

The three distinct tool-workpiece interface surfaces are tool shoulder, tool pin side, and tool pin tip. However, the contribution of tool tip surface is negligible (Ref. 30) toward the total heat generation required for welding. $Q_1$ and $Q_2$ are the components of the respective heat generated from the tool shoulder and tool pin side interfaces, as shown in Fig. 1. Therefore, the total heat generated is given by $Q_{total} = Q_1 + Q_2$.

### Tool Shoulder - Workpiece Interface

The expressions were derived considering a concave shoulder surface. The purpose of this geometric feature is to act as an escape volume as the tool pin is plunged into the plate during the welding operation.

The concave shoulder surface is represented by its vertical and horizontal projected surfaces as $A_V$ and $A_H$, respectively. Therefore, for an elemental segment

$$\begin{aligned} & dA_V = r\ d\theta\ dz \\ \text{now} \quad & dz = \tan\alpha\ dr, \\ \text{therefore,} \quad & dA_V = r\ d\theta\ \tan\alpha\ dr \\ \text{and} \quad & dA_H = r\ d\theta\ dr. \end{aligned}$$

The forces acting on the tool shoulder can be written as

$$\begin{aligned} dF_s &= \mu p\left(dA_H + dA_V\right) \\ &= \mu p\ r\ d\theta\ dr(1+\tan\alpha) \end{aligned} \qquad (7)$$

From Equation 7 one can observe that the concave shoulder surface actually contributes to increased frictional area by a factor of tan α.

Therefore, combining Equations 6 and 7, the heat generation from the elemental shoulder surface is given by

$$\begin{aligned} dQ_S &= \omega\ r\ dF_S \\ &= \omega r^2\ \mu p\ d\theta\ dr(1+\tan\alpha) \end{aligned} \qquad (8)$$

The heat generated through friction of the tool shoulder with the plate surface is obtained by integrating Equation 8 from the pin root radius to the outer radius of the shoulder surface.

$$\begin{aligned} Q_1 &= \int_0^{2\pi}\int_{R_p}^{R_S} \omega \mu p r^2 (1+\tan\alpha)\, dr\ d\theta \\ &= \frac{2}{3}\pi \mu p \omega \left(R_S^3 - R_p^3\right)(1+\tan\alpha) \end{aligned} \qquad (9)$$

### Tool Pin-Workpiece Interface

Heat generated from the cylindrical tool pin side surface is denoted by $Q_2$. As the FSW tool traverses along the joint, the forward half of the tool pin experiences a reaction force F as shown in Fig. 2. It is the

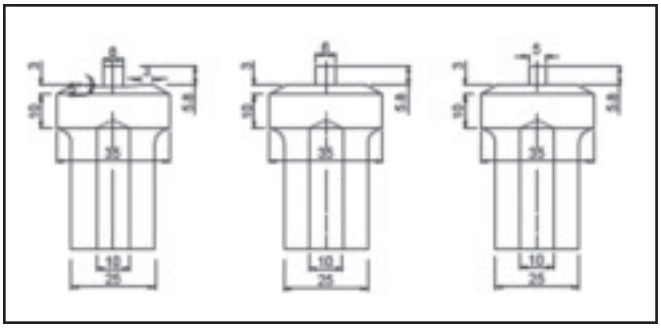

*Fig. 3 — Details of tool geometry with cylindrical tool pin.*

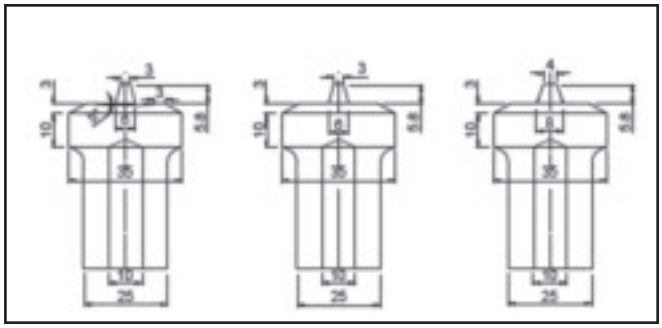

*Fig. 4 — Details of tool geometry with conical tool pin.*

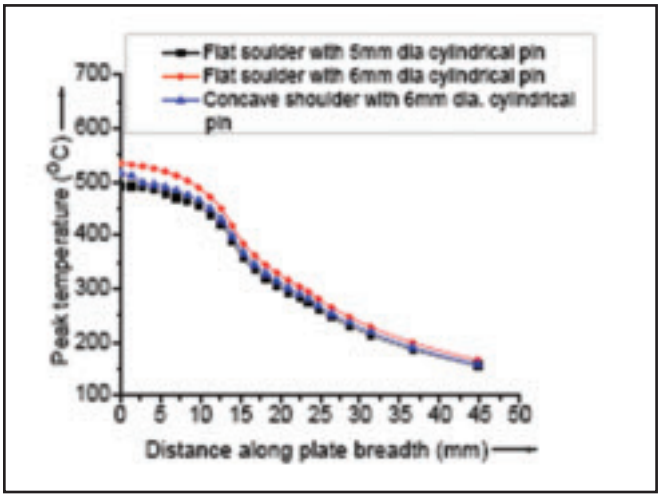


*Fig. 5 — Peak temperature distribution along plate breadth perpendicular to the weld interface using cylindrical pin.*

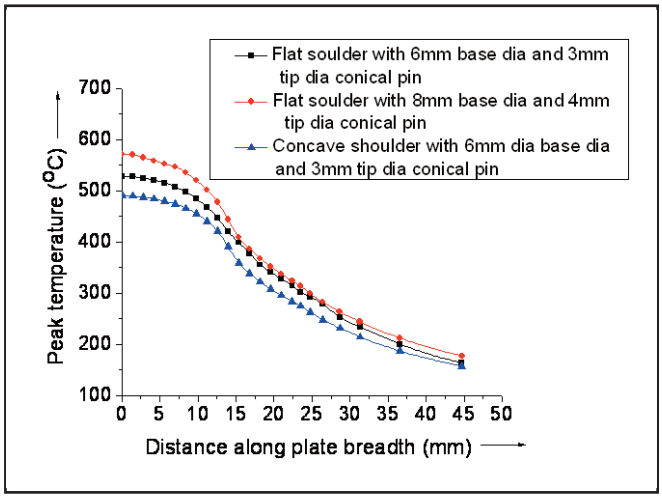


*Fig. 6 — Peak temperature distribution along plate breadth perpendicular to the weld interface using conical pin.*

product of the projected area of the tool pin and the yield stress of the aluminum alloy at the prevailing temperature of pin-plate interface as given in Equation 10. The temperature at the pin-plate interface was taken as about 80% of the melting temperature of the plate material, i.e. , 530°C.

$$\therefore F = \left(h_p \times d_p\right) \times \left(\sigma_y\right)_{530°C} \quad (10)$$

Therefore, the frictional force experienced by the tool pin side vertical surface will be given as

$$F_V = \left(\mu\right)_{530°C} \times F \quad (11)$$

Hence, the heat generated due to friction of the tool pin side surface will be

$$Q_2 = \omega R_p F_V \quad (12)$$

Therefore, the total heat generation considering pure friction of tool shoulder and pin side surface will be given by

$$Q_{total} = Q_1 + Q_2 = \frac{2}{3}\pi\mu p\omega\left(R_S^3 - R_P^3\right)\left(1+\tan\alpha\right) + \omega R_P F_v \quad (13)$$

In case of a flat shoulder, the heat generation expression simplifies to

$$Q_{total} = \frac{2}{3}\pi\ \mu p\omega\left(R_S^3 - R_P^3\right) + \omega R_P F_v \quad (14)$$

Using the parameters given in Table 1, the calculated values of $Q_1$ and $Q_2$ were found to be 1782 J/s (i.e., 89% of total heat input) and 219 J/s (i.e., 11% of total heat input), respectively. The percentage of heat generation obtained from the above formulation matched well with that of published results (Ref. 30).

## Three-Dimensional Finite Element Model

A three-dimensional FE transient thermal model was developed to determine the thermal history on the workpiece based on the $Q_1$ and $Q_2$ given by Equations 9 and 12, respectively. The following assumptions were made in the analysis:

1) All the thermal properties of AA1100 were considered as a function of temperature.

2) Linear Newtonian convection cooling was considered on all the surfaces.

**Table 1 — Typical FSW Parameters**

| Thickness of Plates (mm) | Tool Pin Diameter (mm) | Shoulder Diameter (mm) | Rotational Speed (rpm) | Traverse Speed (mm/min) | Average Plunging Force on FSW Tool during Welding (N) |
|---|---|---|---|---|---|
| 6.0 | 6.0 | 25.0 | 1400 | 112 | 5090 |

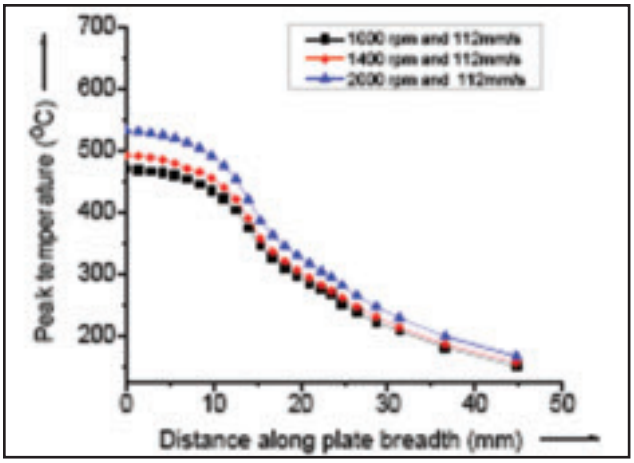


*Fig. 7 — Variation of peak temperature distribution with tool rotational speed.*

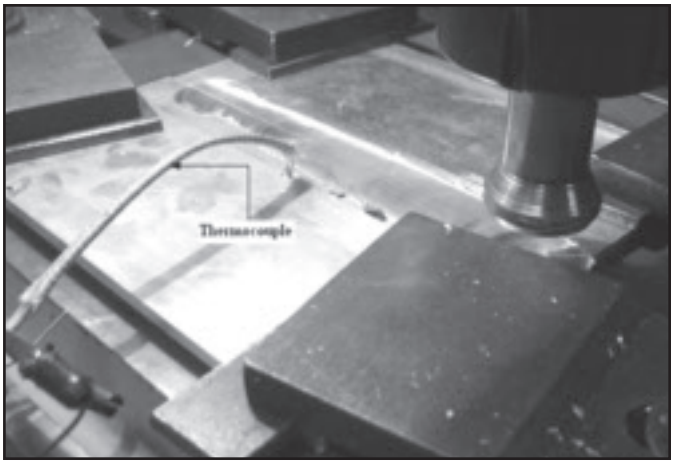


*Fig. 8 — Experimental setup of FSW process.*

3) 95% of the heat was transferred to the workpiece.

The governing differential equation is

$$\frac{\partial}{\partial x}\left[K\frac{\partial T}{\partial x}\right]+\frac{\partial}{\partial y}\left[K\frac{\partial T}{\partial y}\right]+\frac{\partial}{\partial z}\left[K\frac{\partial T}{\partial z}\right]=\rho\, C\frac{\partial T}{\partial t} \quad (15)$$

The boundary conditions below were applied in the present FE model.

**Table 2 — Temperature-Dependent Properties of Aluminum Alloy**

| Temperature °C | Thermal Conductivity W/m°C | Heat Capacity J/Kg°C |
|---|---|---|
| 37.8 | 162 | 945 |
| 93.3 | 177 | 978 |
| 148.9 | 184 | 1004 |
| 204.4 | 192 | 1028 |
| 260 | 201 | 1052 |
| 315.6 | 207 | 1078 |
| 371.1 | 217 | 1104 |
| 426.7 | 223 | 1133 |

**Table 3 — Temperature-Dependent Friction Coefficient of Aluminum and Steel Combination**

| Temperature (°C) | Friction Coefficient, μ |
|---|---|
| 22 | 0.11 |
| 160 | 0.11 |
| 200 | 0.26 |
| 400 | 0.35 |
| 580 | 0.47 |

### Initial Condition

A specified initial temperature for the entire plate,

$$T = T_\infty \text{ for } t = 0 \quad (16)$$

### First Boundary Condition

A specific heat flow acting over weld surface for $t > 0$ representing the FSW heating source $q_n = -q_{sup}$. The quantity $q_{sup}$ is the heat flux supplied to the plate due to friction at the tool-plate interface. $q_n$ is the normal component of heat flux vector. Here $q_{sup}$ was given by Equation 17.

### Second Boundary Condition

$q_{conv}$ represents the heat loss due to convection from the plate surface at temperature T. Considering $h_f$ as convection coefficient, the heat loss $q_{conv}$ is given by $q_{conv} = h_f (T - T_\infty)$. Considering heat loss due to convection over the top and bottom surface (Newton's law of cooling) $q_n = q_{conv}$ or $-k\,\partial T/\partial n = h_f (T - T_\infty)$ for $t > 0$. It should be noted that heat flux $q_{sup}$ and convection loss $q_{conv}$ do not occur over the same boundary segment at the same time. Heat flow into the boundary is taken as positive.

### Heat Source Model

The heat source modeling was done based on the following assumptions:

1) The heat input is linearly proportional to the distance from the center of the tool.

2) The plunging force applied to the plate surface by the tool creates a uniform pressure over the shoulder surface.

3) The heat is generated from the work done by the friction force only.

The distribution of heat flux (Ref. 26) over the plate surface due to the tool shoulder was given as

$$q(r) = \frac{3Q_1 r}{2\pi R_S^3} \quad \text{for } r \le r_0 \quad (17)$$

The distribution of heat flux over the pin-plate interface due to tool pin side surface was given as

$$q_p = \frac{Q_2}{(A)_{ps}} \quad (18)$$

Where $(A)_{ps}$ is the area of the tool pin side surface.

## Material Properties

The temperature-dependent thermal properties (Ref. 27) of the aluminum alloy used in this analysis are given in Table 2. Constant convection coefficient, 30 W/m²°C was used (Ref. 28) in the analysis. The temperature-dependent friction coefficient of aluminum and steel combination (Refs. 26, 27) is given in Table 3. The melting temperature of AA1100 was taken as 660°C.

## FE Results and Discussion

Transient thermal analysis of FSW of AA1100 was carried out considering two different sets of FSW tools having cylindrical- and conical-shaped tool pins as shown in Figs. 3 and 4, respectively. Brick elements with fine meshing in the weld zone were considered.

The vertical tool plunging force was measured using a load pad. It was ob-

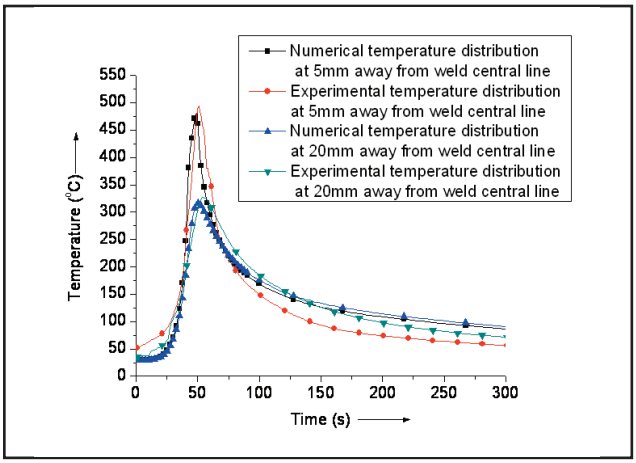


*Fig. 9 — Numerical and experimental temperature distribution at 5 and 20 mm away from the weld center.*

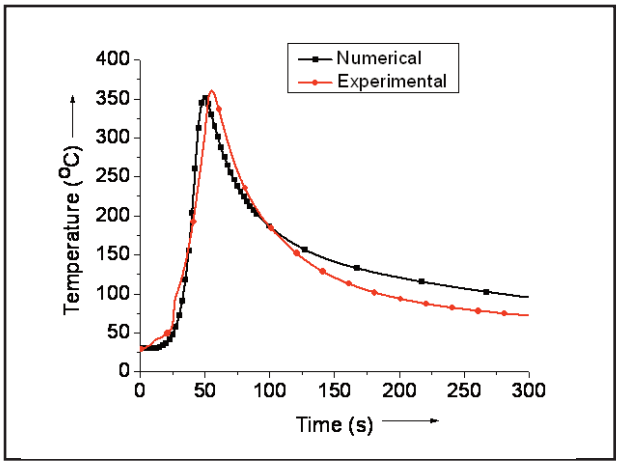


*Fig. 10 — Numerical and experimental temperature distribution for welding with conical tool pin.*

served that the average plunging force required for cylindrical and conical tool pin varied with tool rotational speed. The measured values of plunging force for varying tool rotational speed are given in Table 4.

The peak temperatures obtained from the results of thermal analysis of FSW of AA1100 considering traverse speed of 112 mm/min and tool rev/min of 1400 for different tool geometries are given in Table 5. It can be observed that tools having a concave shoulder led to lesser temperature rise. At the same time, conical tool pins exhibited somewhat lesser peak temperature compared to that of a cylindrical pin having a pin diameter the same as the base diameter of conical pins.

The variations of calculated peak temperature distributions for two sets of three different tool geometries with cylindrical and conical tool pins at traverse speed of 112 mm/min and 1400 rev/min are shown in Figs. 5 and 6, respectively.

From Fig. 5 one can observe that with 1 mm increase in pin diameter peak temperature increased by about 10%. However, with the same pin diameter but with a concave shoulder surface there was about 4.6% reduction in the peak temperature compared to that of flat shoulder surface.

As expected, welding with the tool pin having a higher base diameter led to higher temperature. Also, a reduction in temperature was observed in the case of the tool with concave shoulder.

Figure 7 shows the variation of peak temperature distribution along plate breadth perpendicular to the weld interface for varying tool rotational speeds for a tool having a 5-mm-diameter cylindrical pin with flat shoulder.

Here one can observe that with 100% increase in tool rev/min, i.e., from 1000 to 2000, the increase in peak temperature was only about 13%. It is important to note that although heat generation depends on tool rotational speed, its effect is rather marginal.

## Experimental Details

Extensive experiments with excellent repeatability were carried out to test and val-

**Table 4 — Vertical Plunging Force at Varying Tool Rotational Speeds**

| Thickness of Plates (mm) | Rotational Speed (rpm) | Traverse Speed (mm/min) | Average Plunging Force on FSW Tool during Welding (N) |
|---|---|---|---|
| 6.0 | 1000 | 112 | 6450 |
| 6.0 | 1400 | 112 | 5090 |
| 6.0 | 2000 | 112 | 3800 |

**Table 5 — Peak Temperatures for Different Tool Geometries**

| Sl. No. | | Tool Type | Peak Temperature (°C) | % of Melting Temperature |
|---|---|---|---|---|
| 1 | Cylindrical Pin | Flat shoulder, pin dia. 5 mm | 490 | 74 |
| 2 | | Flat shoulder, pin dia. 6 mm | 540 | 81.8 |
| 3 | | Flat shoulder, pin dia. 8 mm | 598 | 90.6 |
| 4 | | Concave shoulder, pin dia. 5 mm | 462 | 70 |
| 5 | | Concave shoulder, pin dia. 6 mm | 515 | 78.1 |
| 6 | | Concave shoulder, pin dia. 8 mm | 577 | 87.4 |
| 7 | Conical Pin | Flat shoulder, pin base dia. 5 mm, tip dia. 2.5 mm | 479 | 72.58 |
| 8 | | Flat shoulder, pin base dia. 6 mm, tip dia. 3 mm | 528 | 80 |
| 9 | | Flat shoulder, pin base dia. 8 mm, tip dia. 3 mm | 571 | 86.5 |
| 10 | | Concave shoulder, pin base dia. 5 mm, tip dia. 2.5 mm | 457 | 70 |
| 11 | | Concave shoulder, pin base dia. 6 mm, tip dia. 3 mm | 491 | 74.4 |
| 12 | | Concave shoulder, pin base dia. 8 mm, tip dia. 4 mm | 554 | 84 |

Tool traverse speed = 112 mm/min, Tool rpm = 1400

idate the numerical model for calculating the thermal history of FSW of AA1100.

A vertical milling machine with only 7.5 - hp motor capacity was used to carry out the FSW experiments. The tools were mounted in the vertical arbor using suitable collates. The edges of the test pieces were machined to obtain a neat square butt. They were clamped to the horizontal bed with zero root opening. The butt line was aligned with the centerline of the FSW tool. The clamping of the test pieces was done such that the movement of the plates was totally restricted under both plunging and translational forces of the FSW tools. The tool rev/min and translational speed of the bed were set prior to each run of welding. After plunging the rotating tool at the plate butt joint and visually ensuring full contact of the tool shoulder with the plate surface, the bed horizontal movement was switched on. A typical FSW setup is shown in Fig. 8. The FSW tools were fabricated in house using SS310.

For measuring temperature distribution during welding, thermocouples were used 5 and 20 mm away from the weld interface on bottom and upper surfaces of the plates respectively, as shown in Fig. 8. Thermocouples were used at the middle length of the plate along the longitudinal direction as shown in Fig. 8. Agilent data logger 34970A was used to record temperature data. For measurement of tool plunging force, a 5000-kg-capacity load pad was used.

Several test samples 300 mm long and 200 mm wide taken from 6-mm-thick AA1100 plate were welded with the above referred FSW tools.

## Experimental Results

Several experiments with temperature measurements were conducted. The numerical and experimental temperature distribution for welding with flat shoulder tools having 5- and 6-mm-diameter cylindrical tool pins were plotted as shown in Fig 9. The welding was carried out with tool traverse and rotational speed of 112 mm/min and 1400 rev/min respectively.

Figure 10 shows a sample result of numerical and experimental temperature distribution for welding with a conical tool having an 8-mm root diameter and 4-mm tip diameter with concave shoulder. The temperature was recorded 20 mm away from the center of the weld interface. The welding was carried out with tool rotational and transverse speeds of 1400 rev/min and 112 mm/min, respectively.

The measured thermal history compared well with the calculated ones as can be seen in Figs. 9 and 10. Some mismatch can be observed in the cooling rate below about 150°C. However, more importantly, the peak temperatures measured, which have major influence on the overall welding process, were found to be in very good agreement with the calculated ones. A variation of about 2.4 to 3.3% from the measured data was noted. Hence, it points to the fact that in FSW of AA1100 with a SS310 tool, friction is the major contributor to heat generation.

It was observed that the tendency of a wormhole defect to occur toward the bottom of the weld increased when the diameter of the tool pin increased in the case of cylindrical tools and increasing base diameter with conical tool pins, irrespective of tool rotational or traverse speed. A higher diameter tool pin implies a higher volume of material displacement, and thus, it may lead to inadequate material flow toward the bottom of the weld, causing a wormhole defect.

## Conclusions

The thermal history obtained through the model developed in the present study compared fairly well with the experimentally measured thermal profile at two different locations. Variation in peak temperature at these two locations was found to be only about 2.4 to 3.3%. Hence, it points to the fact that in FSW of AA1100 with a SS310 tool, friction is the major contributor to heat generation.

It was observed that tools having a concave shoulder led to lesser temperature rise. At the same time, conical tool pins exhibited somewhat lesser peak temperature compared to that of a cylindrical pin having a pin diameter the same as the base diameter of conical pins. The calculated peak temperatures were all closer to or more than about 80% of the liquidus temperature of AA1100. Therefore, tool geometry with a concave shoulder and conical pin is preferable for FSW of AA1100.

For a particular welding parameter, the peak temperature increased only around 10% for the cylindrical pin when its diameter increased by 1 mm. Since the increase in pin diameter does not significantly contribute to heat generation, it is preferable to keep its diameter as low as possible providing for adequate bending and shearing strength of the tool pin. Extensive experiments were carried out and it was observed that a lower tool pin diameter resulted in good weld quality.

With 100% increase in tool rev/min, i.e., from 1000 to 2000 rev/min, the increase in peak temperature was only about 13%. Although heat generation depends on tool rotational speed, its effect is rather marginal. However, with a 100% increase in tool rev/min, the reduction of plunging force was more than 40%, which justifies use of higher tool rev/min.

*Acknowledgments*

The authors sincerely acknowledge the funding support from Naval Research Board to carry out the research, and also the generous help extended by Garden Reach Shipbuilders and Engineers Ltd., Kolkata, by providing AA1100 to carry out the experiments.

*References*

1. Chao, Y. J., Qi, X., and Tang, W. 2003. Heat transfer in friction stir welding — Experimental and numerical studies, *Transaction of the ASME*, pp. 125, 138–145.

2. Nandan, R., DebRoy, T., and Bhadeshia, H. K. D. H. 2008. Recent advances in friction stir welding — Process, weldment structure and properties. *Progress in Materials Science* 53: 980–1023.

3. London, B., Mahoney, M., Bingel, B., Calabrese, M., and Waldron, D. 2001. *Proceedings of the Third International Symposium on Friction Stir Welding*. Kobe, Japan.

4. Colegrove, P. A., and Shercliff, H. R. 2004. Development of Trivex friction stir welding tool part 1 — two-dimensional flow modelling and experimental validation. *Science and Technology of Welding and Joining* 9: 345–351.

5. Colegrove, P. A., and Shercliff, H. R. 2004. Development of Trivex friction stir welding tool part 2 — three-dimensional flow modeling. *Science and Technology of Welding* 9: 352–361.

6. Biswas, P., and Mandal, N. R. 2009. Experimental study on friction stir welding of marine grade aluminum alloy. *Journal of Ship Production* 25(1), 1–6.

7. Song, M., and Kovacevic, R. 2002. A new heat transfer model for friction stir- welding. *transaction of NAMRI/SME, SME* 30: 565–572.

8. Song, M., and Kovacevic, R. 2003. Thermal modeling of friction stir welding in a moving coordinate system and its validation. *Int. J. of Machine Tools & Manufacture* 43: 605–615.

9. Schmidt, H., Hattel, J., and Wert, J. 2004. An analytical model for the heat generation in friction stir welding. *Modeling and Simulation in Materials Science and Engineering* 12: 143–157.

10. Gould, J. E., and Feng, Z. 1998. Heat flow model for friction stir welding of aluminum alloys. *Journal of Materials Processing & Manufacturing Science* 7(2):185–194.

11. Chao, Y. J., and Qi, X. 1998. Thermal and thermo-mechanical modeling of friction stir welding of aluminum alloy 6061-T6. *Journal of Materials Processing & Manufacturing Science,* 7(2): 215–233.

12. Chao, Y. J., Qi, X., and Tang, W., 2003. Heat transfer in friction stir welding — experimental and numerical studies. *ASME Journal of Manufacturing Science and Engineering* 125(1): 138–145.

13. Frigaard, O., Grong, O., Bjorneklett, B., and Milding, O. T. 1999. Modeling of the thermal and microstructure field during friction stir welding of aluminum alloys. *1st International Symposium on Friction Stir Welding*, Thousand Oaks, Calif.

14. Frigaard, O., Grong, O., and Milding, O. T. 1998. Modeling of heat flow phenomena in friction stir welding of aluminum alloys. *Proceeding of the INALCO'98*, Cambridge, UK.

15. Song, M., and Kovacevic, R. 2002. A new

heat transfer model for friction stir welding. *Transactions of NAMRI/SME*, Vol. XXX, No. MS02-175, 565–572.

16. Song, M., Ouyang, J. H., and Kovacevic, R. 2003. Numerical and experimental study of heat transfer during friction stir welding of aluminum alloy 6061-T6. *Proceeding of the Institute of Mechanical Engineers, Part B, Journal of Engineering Manufacture* 217(1): 73–85.

17. Ulysse, P. 2002. Three-dimensional modeling of friction stir-welding process. *Machine Tools & Manufacture* 42, 1549–1557.

18. Chen, C. M., and Kovacevic, R. 2003. Finite element modeling of friction stir welding — thermal and thermo-mechanical analysis. *Machine Tools & Manufacture* 43: 1319–1326.

19. Colegrove, P. A., Painter, M., Graham, D., and Miller, T. 2002. 3 Dimensional flow and thermal modeling of the friction stir welding process. *2nd International Symposium on Friction Stir Welding*, Gothenburg, Sweden, pp. 26–28.

20. Dong, P., Lu, F., Hong, J. K., and Cao, Z. 2001. Coupled thermomechanical analysis of friction stir welding process using simplified models. *Science and Technology of Welding and Joining* 6(5): 281–287.

21. Shi, Q. Y., Dickerson, T., and Shercliff, H. R. 2003. Thermo-mechanical FE modeling of friction stir welding of Al-2024 including tool loads. *4th International Symposium on Friction Stir Welding*, Park City, Utah.

22. Nandan, R., Roy, G. G., and Deb- Roy, T. 2006. Numerical simulation of three-dimensional heat transfer and plastic flow during friction stir welding. *Metallurgical and Materials Transaction* A 37(4): 1247–59.

23. Nandan, R., Roy, G. G., Lienert, T., and DebRoy, T. 2006. Numerical modelling of 3D plastic flow and heat transfer during friction stir welding of stainless steel. *Science and Technology of Welding and Joining*, 11(5): 526–537.

24. Nandan, R., Roy, G. G., Lienert, T., and DebRoy, T. 2007. Three-dimensional heat and material flow during friction stir welding of mild steel. *Acta Materialia* 55: 883–895.

25. Bastier, M. H., Maitournam, K.van Dang, and Roger, F. 2006. Steady state thermomechanical modelling of friction stir welding. *Science and Technology of Welding and Joining* 11: 278–288.

26. Chao, Y. J., and Qi, X. 1998. Thermal and thermo-mechanical modeling of friction stir welding of aluminum alloy 6061-T6. *Journal of Materials Processing & Manufacturing Science* 7: 215–233.

27. Wong, J. C. 2008. The Correspondence between Experimental Data and Computer Simulation of Friction Stir Welding (FSW). Master of Science in Mechanical Engineering, Department of Mechanical and Aerospace Engineering, Morgantown, W. V.

28. Chao, Y. J., Qi, X., and Tang, W. 2003. Heat transfer in friction stir welding-experimental and numerical studies. *Transactions of the ASME*, 125, 138–145.

29. *Metals Handbook*. 1979. Ninth edition, Vol. 2, ASM International, p. 104.

30. *Friction Stir Welding*. 2010. D. Lohwasser and Z. Chen, eds., Woodhead Publishing Ltd., pp. 282 and 309.

### Nomenclature

$\alpha$ = shoulder concavity angle

$\delta$ = extent of slip

$\rho$ = II density of plate material

$\mu$ = coefficient of friction

$\tau_y$ = shear yield stress

$\omega$ = tool angular rotational speed

$c$ = specific heat

$dA$ = elemental area

$k$ = thermal conductivity

$p$ = tool plunging pressure applied on the elemental area $dA$

$r$ = length along tool radius

$A_H$ = horizontal projected surfaces area

$A_V$ = vertical projected surfaces area

$Q$ = heat input to the workpiece

$Q_1$ = heat generated under the tool shoulder

$Q_2$ = heat generated at the tool pin side

$Q_3$ = heat generated at the tool pin tip

$Q_{total}$ = total heat generated

$R_P$ = pin root radius

$R_S$ = outer radius of shoulder surface

$T_\infty$ = ambient temperature

## Authors: Submit Research Papers Online

**Peer review of research papers is now managed through an online system using Editorial Manager software. Papers can be submitted into the system directly from the Welding Journal page on the AWS Web site (www.aws.org) by clicking on "submit papers." You can also access the new site directly at www.editorialmanager.com/wj/. Follow the instructions to register or login, and make sure your information is up to date. This online system streamlines the review process, and makes it easier to submit papers and track their progress.**

**By publishing in the Welding Journal, more than 66,000 members will receive the results of your research. Additionally your full paper is posted on the American Welding Society Web site for FREE access around the globe. There are no page charges, and articles are published in full color. By far, the most people, at the least cost, will recognize your research when you publish in the world-respected Welding Journal.**